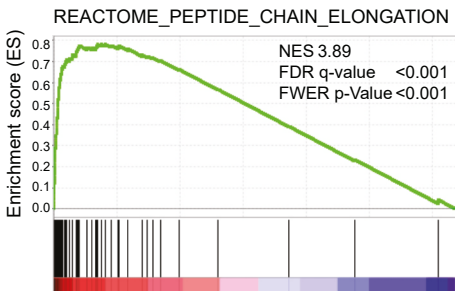


A

Geneset	NES	NOM p-value	FDR q-value
REACTOME_NONSENSE_MEDIATED_DECAY_ENHANCED_BY_THE_EXON_JUNCTION_COMPLEX	3.9	0	0
REACTOME_PEPTIDE_CHAIN_ELONGATION	3.89	0	0
MIPS_RIBOSOME_CYTOPLASMIC	3.85	0	0
REACTOME_INFLUENZA_VIRAL_RNA_TRANSCRIPTION_AND_REPLICATION	3.82	0	0
REACTOME_SRP_DEPENDENT_COTRANSLATIONAL_PROTEIN_TARGETING_TO_MEMBRANE	3.81	0	0
REACTOME_3_UTR_MEDIATED_TRANSLATIONAL_REGULATION	3.81	0	0
REACTOME_TRANSLATION	3.79	0	0
BILANGES_SERUM_AND_RAPAMYCIN_SENSITIVE_GENES	3.78	0	0
REACTOME_METABOLISM_OF_MRNA	3.75	0	0
KEGG_RIBOSOME	3.75	0	0

B



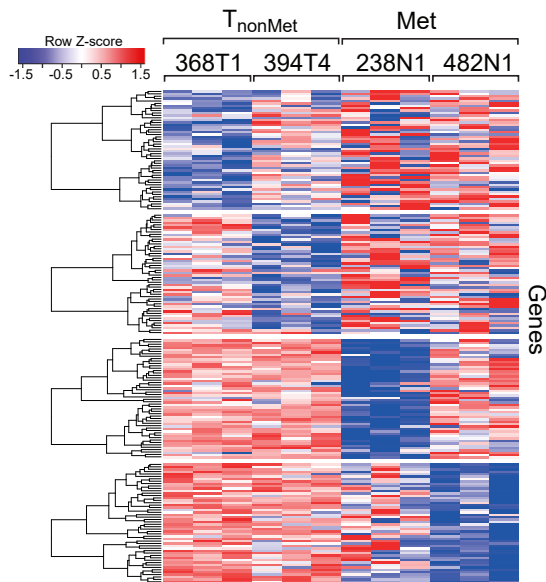
C

GO Term	p-value
translation	1.70E-39
RNA processing	3.30E-10
ribonucleoprotein complex biogenesis	5.90E-08
RNA splicing	9.30E-08
mRNA metabolic process	2.90E-07
ribosome biogenesis	4.20E-07
mRNA processing	5.20E-07
translational initiation	2.20E-05
rRNA processing	3.20E-05
rRNA metabolic process	3.70E-05
protein localization	8.30E-05
protein transport	8.70E-05
cell cycle	1.00E-04

D

shRNA	T _{nonMet}		Met	
	368T1	394T4	238N1	482N1
<i>Cdkn2a</i>	2.96	0.34	1.96	2.04
<i>Nf2</i>	3.11	1.71	3.37	1.22
<i>Rb1</i>	1.95	2.27	3.39	3.00
<i>Tsc2</i>	1.86	2.23	3.90	4.32
<i>Cdkn2b</i>	3.06	3.59	4.30	4.60

E



Supplementary Figure S1. A genome-scale shRNA screen identifies candidate metastasis-specific lethal genes

A. Gene set enrichment analysis (GSEA) of genes that lose representation in all cell line samples during *in vitro* culture uncovers many known essential pathways. The pathways eliciting the most broadly lethal shRNA treatment responses are shown.

B. An example of a broadly essential pathway. Vertical bars are genes represented in the gene set/pathway sorted by essentiality (left: more essential) and the enrichment score is graphed above (green trace).

C. Gene ontology (GO) analysis depicts that knockdown of genes in essential pathways leads to reduced representation in all cell lines.

D. Single shRNAs targeting known tumor suppressors are within the most enriched shRNA across all cell lines. Numbers indicate log₂ fold change in loss of representation in the late samples.

E. Top 50 genes that are specifically required for each cell line, where knockdown leads to reduced representation in each individual cell line. Heatmaps show the Weighted Sum metric of shRNA representation for each gene after knockdown. Panels show cell-line specific lethal genes for (from top) 368T1, 394T4, 238N1, and 482N1 respectively.

A

Lethal to all

12 genes
2 shRNAs per gene

Mtor
Eif4g1
Mcm6
Cse1l
Wee1
Nsf
Pdpk1
Eif3c
Rps3
Rps4x
Snrpe
Snrpd3

Advantageous to all

5 genes
1 shRNA per gene

Nf2
Rb1
Tsc2
Cdkn2b
Ccnc

Inert

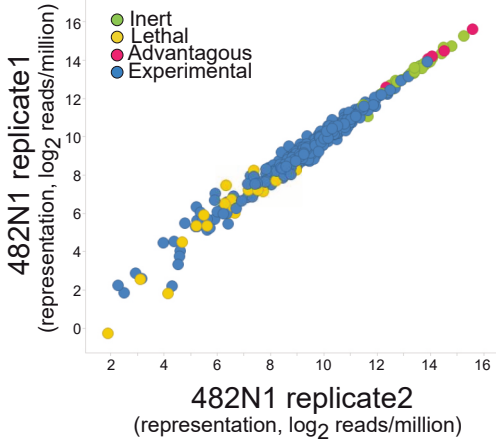
comprizing 20% of the total pool
32 shRNAs

Metastasis Lethal

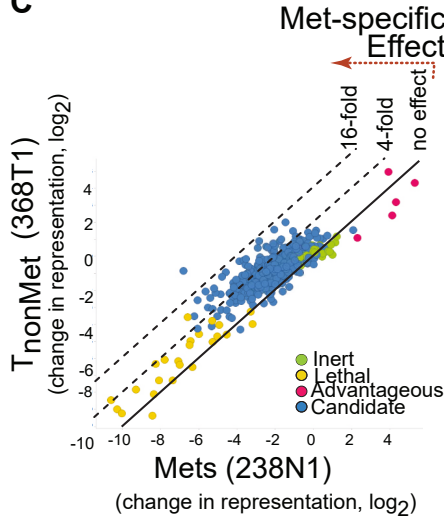
240 genes
1-2 shRNAs per gene

<i>Klf5</i>	<i>Mrpl14</i>	<i>Gls2</i>	<i>Mrps27</i>	<i>Zmym5</i>	<i>Fam102b</i>	<i>Mrpl30</i>	<i>Fbxo32</i>	<i>Cdhr5</i>
<i>Mdp1</i>	<i>Mtif3</i>	<i>Sp1</i>	<i>Cryab</i>	<i>Mbtd1</i>	<i>Ghr</i>	<i>Hmgcs1</i>	<i>Mrpl54</i>	<i>Tnfrsf1a</i>
<i>Otud5</i>	<i>Cry1</i>	<i>Limk2</i>	<i>Gabarapl2</i>	<i>Ift52</i>	<i>Mkl1</i>	<i>Slc20a2</i>	<i>Asap1</i>	<i>Mrpl21</i>
<i>Spata24</i>	<i>Klf6</i>	<i>Mrpl19</i>	<i>Ywhae</i>	<i>Hadh</i>	<i>Cd274</i>	<i>Psmc3</i>	<i>Mctp1</i>	<i>Mrpl20</i>
<i>Gspt2</i>	<i>Cldn6</i>	<i>Dap</i>	<i>Tubb5</i>	<i>Adi1</i>	<i>Mettl22</i>	<i>Smad1</i>	<i>Srf</i>	<i>Mapk9</i>
<i>Dnajb4</i>	<i>Fads6</i>	<i>Ap4b1</i>	<i>Arl4c</i>	<i>Lemd2</i>	<i>Smad7</i>	<i>Mia2</i>	<i>Jun</i>	<i>Sypl</i>
<i>Ciz1</i>	<i>Katnb1</i>	<i>Nox4</i>	<i>Ccbl2</i>	<i>Zbtb10</i>	<i>Oxnad1</i>	<i>Gpank1</i>	<i>Abcb1a</i>	<i>Zfp422</i>
<i>Slc7a1</i>	<i>Nln</i>	<i>Mtif2</i>	<i>Scin</i>	<i>Rc3h1</i>	<i>Crkl</i>	<i>Rasgrf2</i>	<i>Atm</i>	<i>Klhl10</i>
<i>Pld1</i>	<i>Tead1</i>	<i>Slc39a9</i>	<i>Gtf2b</i>	<i>Tbc1d9</i>	<i>Ppp3ca</i>	<i>Zfp810</i>	<i>Pik3ca</i>	<i>Setd6</i>
<i>Tpr</i>	<i>Nudt15</i>	<i>Cep350</i>	<i>Lrrc57</i>	<i>Fam96a</i>	<i>Sema6d</i>	<i>Ndufaf4</i>	<i>Ripk2</i>	<i>1810055G02Rik</i>
<i>Npas1</i>	<i>Slc12a9</i>	<i>Sar1b</i>	<i>Fgfr11</i>	<i>Ndufb3</i>	<i>Nudt1</i>	<i>Nktr</i>	<i>Sra1</i>	<i>1810026J23Rik</i>
<i>Ppfi3</i>	<i>Vps11</i>	<i>Ddx3x</i>	<i>Cnot2</i>	<i>Aip</i>	<i>Aox1</i>	<i>Mrpl52</i>	<i>Rac1</i>	<i>8430406I07Rik</i>
<i>Ick</i>	<i>Atpaf1</i>	<i>Fxn</i>	<i>Gtf2h3</i>	<i>Akap12</i>	<i>Mxd1</i>	<i>Ythdc2</i>	<i>Spryd4</i>	<i>2810021B07Rik</i>
<i>Baiap21l</i>	<i>Atp5h</i>	<i>Slc22a18</i>	<i>Tbc1d5</i>	<i>Qrich1</i>	<i>Setd1b</i>	<i>Arpc3</i>	<i>Ddx19b</i>	<i>2310033P09Rik</i>
<i>Mzt2</i>	<i>Nsun4</i>	<i>Bcap29</i>	<i>Dpm2</i>	<i>Lass5</i>	<i>Abhd14b</i>	<i>Mrp63</i>	<i>Ivl</i>	<i>Apat6</i>
<i>Ndr3</i>	<i>Zfp3612</i>	<i>Acvr1b</i>	<i>Rad52</i>	<i>Csf2ra</i>	<i>Wrb</i>	<i>Fkbp8</i>	<i>Whsc2</i>	<i>Tfap2b</i>
<i>Mrpl10</i>	<i>Cyth2</i>	<i>Wasl</i>	<i>Csnk1g3</i>	<i>Pkn2</i>	<i>Tab1</i>	<i>Chrb1</i>	<i>Ikbkg</i>	<i>lpp</i>
<i>Tspo</i>	<i>Rai1</i>	<i>Fam36a</i>	<i>Gca</i>	<i>Anapc2</i>	<i>Thap7</i>	<i>Stk36</i>	<i>Ssx2ip</i>	<i>Epb4.112</i>
<i>Ndufa8</i>	<i>Top3a</i>	<i>Pdha2</i>	<i>Rabep1</i>	<i>Bet1</i>	<i>Mrpl24</i>	<i>Asb8</i>	<i>Eif2ak2</i>	<i>Rpa2</i>
<i>Eif4a1</i>	<i>Magee1</i>	<i>Spp13</i>	<i>Vrk3</i>	<i>Evi5</i>	<i>Rpp38</i>	<i>Csnk2a2</i>	<i>Tcea3</i>	<i>Rabgap1</i>
<i>Smug1</i>	<i>Xrn2</i>	<i>Xpo1</i>	<i>Polm</i>	<i>Hist3h2ba</i>	<i>Ath11</i>	<i>Mrpl39</i>	<i>Tgif2</i>	<i>Ptprk</i>
<i>Crk</i>	<i>Nudc</i>	<i>Plcb1</i>	<i>Vapa</i>	<i>Slx1b</i>	<i>Nfkb1</i>	<i>Nck2</i>	<i>Rps6ka1</i>	<i>Ly6c1</i>
<i>Tnrc18</i>	<i>Car14</i>	<i>Diap2</i>	<i>Rnf125</i>	<i>Phf7</i>	<i>Mrpl42</i>	<i>Lss</i>	<i>Grhl3</i>	<i>Ifi2712b</i>
<i>Gpatch1</i>	<i>Plod2</i>	<i>H13</i>	<i>Ppp5c</i>	<i>Ccdc99</i>	<i>Ywhah</i>	<i>Yme111</i>	<i>Pcdhb22</i>	<i>Acp6</i>
<i>Plcl1</i>	<i>Sipa111</i>	<i>Csnk1g1</i>	<i>Iars2</i>	<i>Letm1</i>	<i>Ccz1</i>	<i>Mrps26</i>	<i>Raf1</i>	<i>Cln8</i>
<i>Ydjc</i>	<i>Rwdd3</i>	<i>Tmem33</i>	<i>Clybl</i>	<i>Anapc5</i>	<i>Ii23a</i>	<i>Wnt7b</i>	<i>Sod2</i>	<i>Ildr1</i>
			<i>Setbp1</i>	<i>Mrpl16</i>	<i>Fam20b</i>	<i>Cd55</i>	<i>Evl</i>	<i>Tagln2</i>

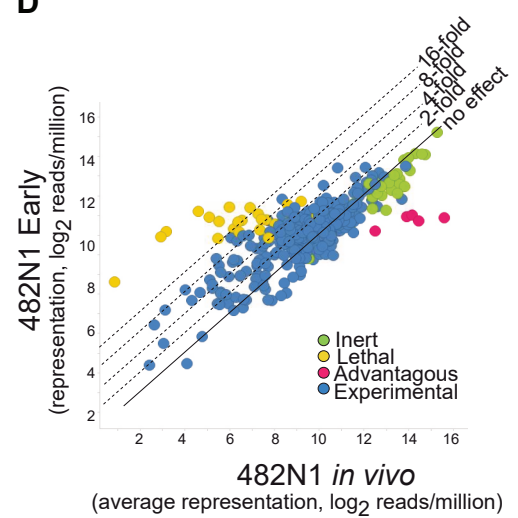
B



C



D



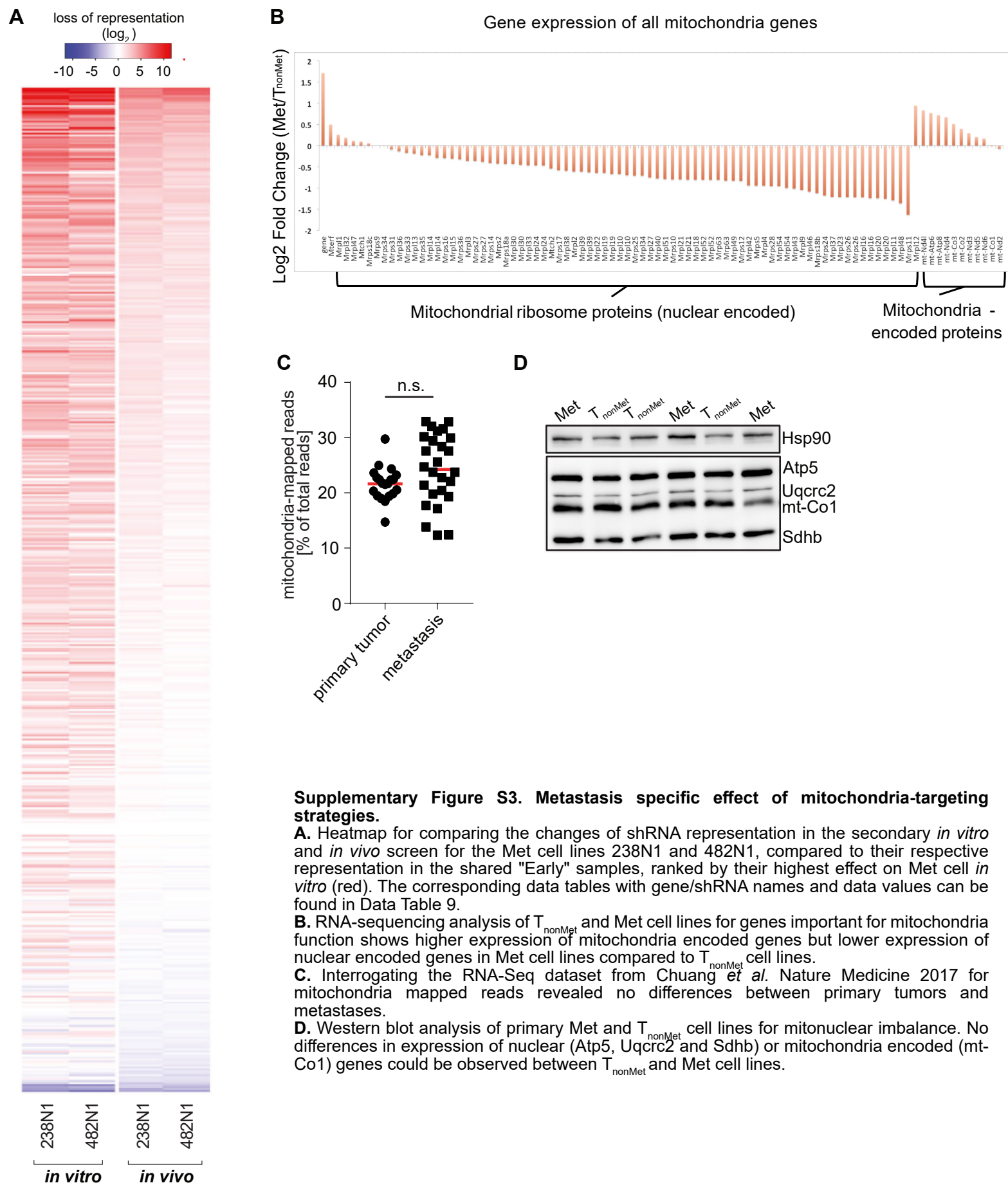
Supplementary Figure S2. Validation of metastasis specific lethal/sick genes

A. List of candidate genes identified in the initial screen and control genes (lethal, advantageous or inert) chosen for the secondary *in vitro* and *in vivo* screen. Genes involved in mitochondria function or metabolism are highlighted in red.

B. Comparison of representation between replicates shows high reproducibility. Each dot represents one shRNA.

C. Differential effect of each shRNA on 238N1 (Met) versus 368T1 (T_{nonMet}) cells. The difference in the change in representation between the Early and Late timepoint is indicated as Met-specific effect with many genes having a > 4x greater effect in the Met cells. Each dot represents one shRNA.

D. Representation before (Early) and after (Late) 20 doubling of 482N1 cells *in vivo*. The representation of lethal genes is reduced, inert genes are unchanged, and advantageous genes increase. Candidate genes have a great reduction in representation in the *in vivo* (Late) cells. Each dot represents one shRNA.



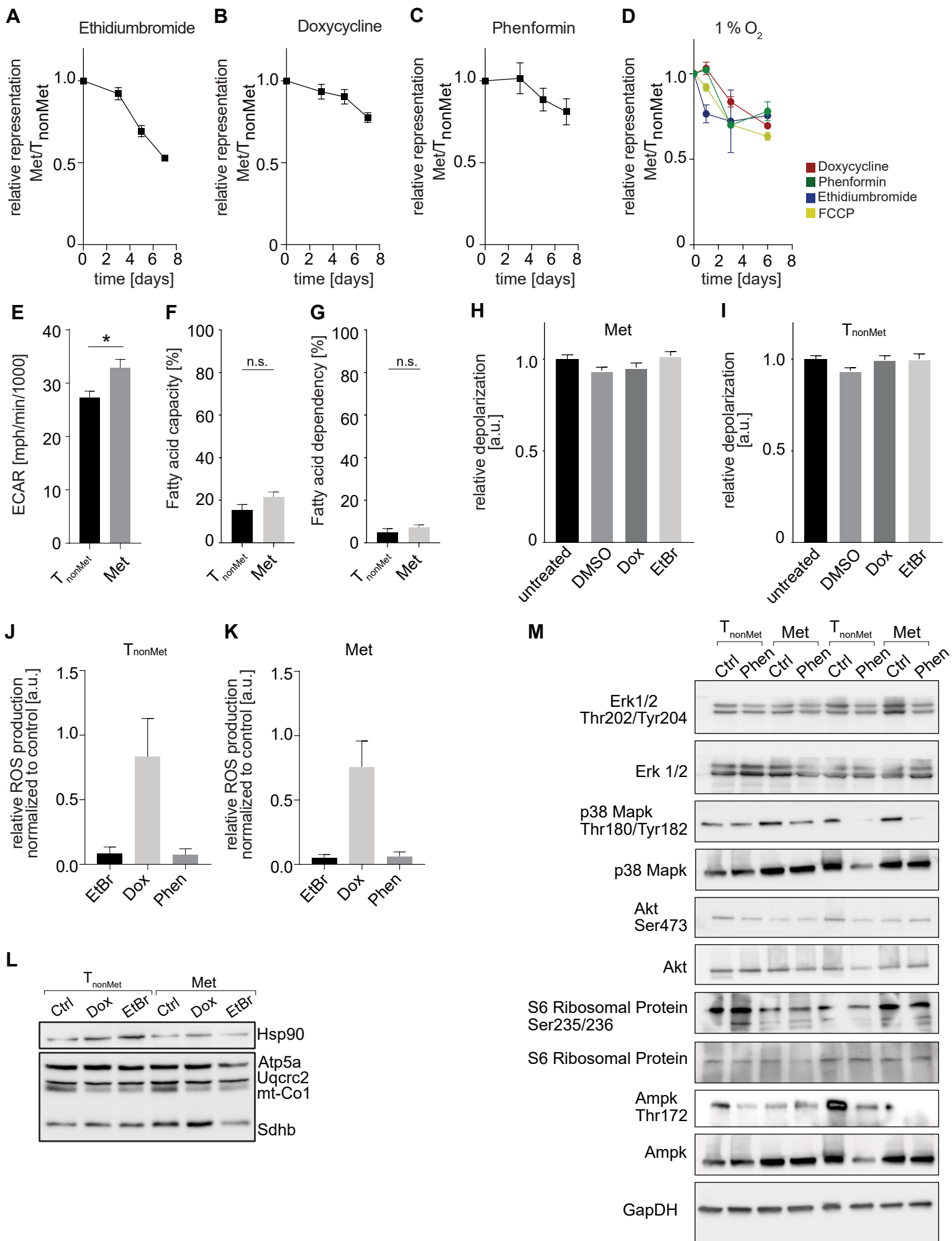
Supplementary Figure S3. Metastasis specific effect of mitochondria-targeting strategies.

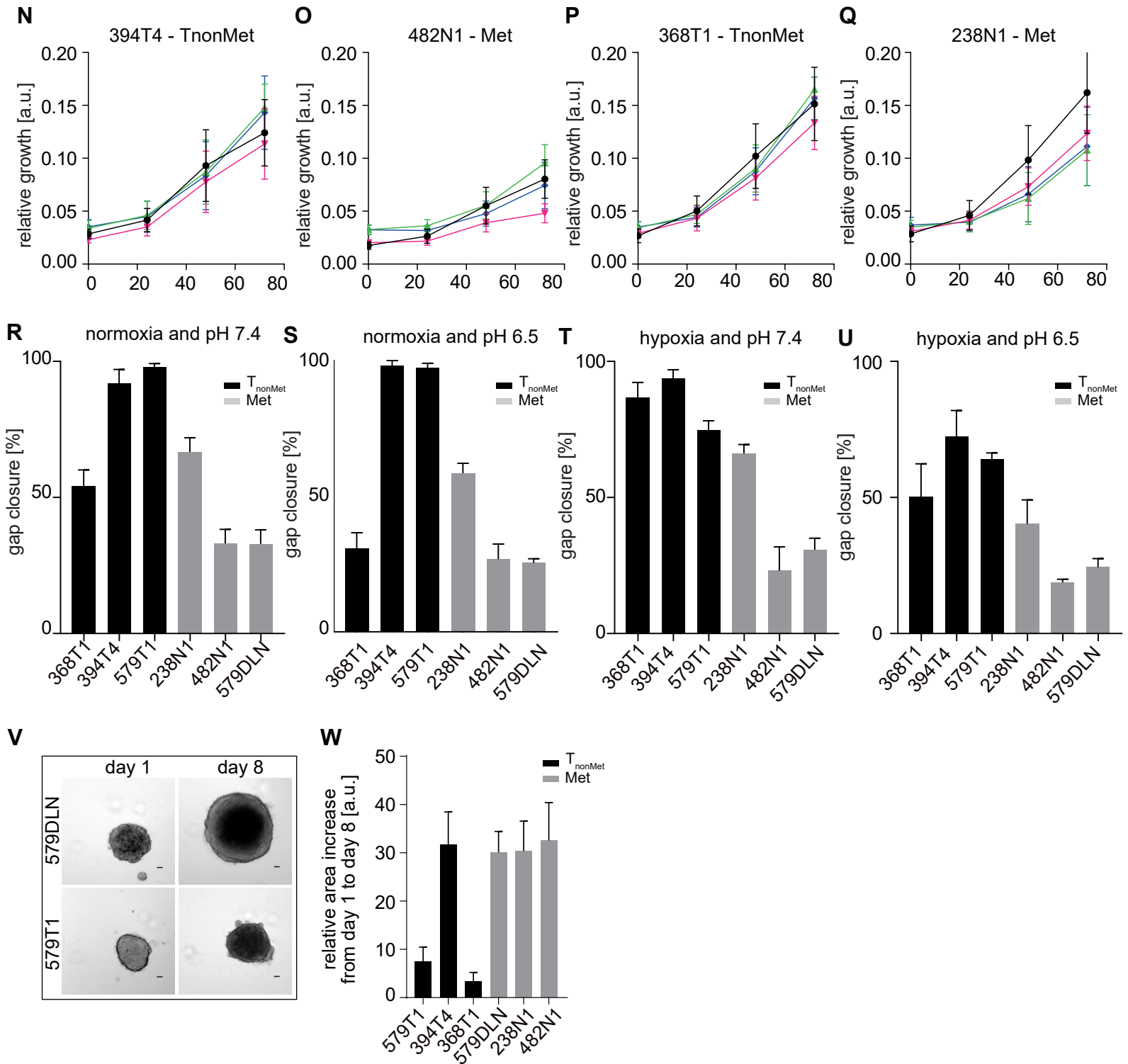
A. Heatmap for comparing the changes of shRNA representation in the secondary *in vitro* and *in vivo* screen for the Met cell lines 238N1 and 482N1, compared to their respective representation in the shared "Early" samples, ranked by their highest effect on Met cell *in vitro* (red). The corresponding data tables with gene/shRNA names and data values can be found in Data Table 9.

B. RNA-sequencing analysis of T_{nonMet} and Met cell lines for genes important for mitochondria function shows higher expression of mitochondria encoded genes but lower expression of nuclear encoded genes in Met cell lines compared to T_{nonMet} cell lines.

C. Interrogating the RNA-Seq dataset from Chuang *et al.* Nature Medicine 2017 for mitochondria mapped reads revealed no differences between primary tumors and metastases.

D. Western blot analysis of primary Met and T_{nonMet} cell lines for mitonuclear imbalance. No differences in expression of nuclear (Atp5, Uqcrc2 and Sdhb) or mitochondria encoded (mt-Co1) genes could be observed between T_{nonMet} and Met cell lines.





Supplementary Figure S4. Metastasis cell lines are more susceptible to mitochondria targeting therapy due to altered mitochondria functionality.

A-C. *In vitro* competition assay of Met (238N1) and T_{nonMet} (368T1) cell lines treated with 50ng/ml ethidium bromide (**A**), 15µg/ml doxycycline (**B**), or 200 µM phenformin (**C**) shows higher treatment effect on Met cells. Data normalized to untreated control; one representative experiment of at least three independent experiments tested in triplicate is shown. Error bars indicate S.D.; if the error bar is missing, the symbol was larger than the error bar.

D. *In vitro* competition assay of Met (482N1) and T_{nonMet} (394T4) cell lines under 1% oxygen conditions treated with 50ng/ml ethidium bromide, 15 µg/ml doxycycline, 200 µM phenformin, or 2 µM FCCP shows higher treatment effect on Met cells. Data normalized to untreated control; one representative experiment of at least three independent experiments tested in triplicate is shown. Error bars indicate S.D.; if the error bar is missing, the symbol was larger than the error bar.

E. Seahorse analysis of Met and T_{nonMet} cell lines (n = 3 each) to measure oxygen consumption rate. Met cell lines show higher ECAR (extracellular acidification rate) indicating higher use of glycolysis in Met cells. Three independent experiments measured in quadruplicate, one representative experiment is shown. Error bars indicate SEM.

F, G. Seahorse MitoFuelFlexTest analysis of Met and T_{nonMet} cell lines (n = 3 each) to measure fuel capacity and dependency. Both T_{nonMet} and Met cells do not seem to fuse or rely on fatty acids as a fuel source. $p > 0.05$, error bars indicate SEM.

H, I. JC1 staining of Met (**H**, n = 2) and T_{nonMet} (**I**, n = 2) cell lines to measure relative depolarization by flow cytometry after treatment with DMSO, doxycycline (Dox) or ethidium bromide (EtBr) normalized to untreated control. No significant differences upon treatment could be observed. Error bars indicate SEM.

J, K. Reactive oxygen species (ROS) staining of T_{nonMet} (**J**) and Met (**K**) cell lines to measure relative ROS production by flow cytometry after treatment with ethidium bromide (EtBr), doxycycline (Dox) or phenformin (Phen) normalized to untreated control. One representative cell line in 3 independent repeats is shown, tested for 2 cell lines each. Error bars indicate SEM.

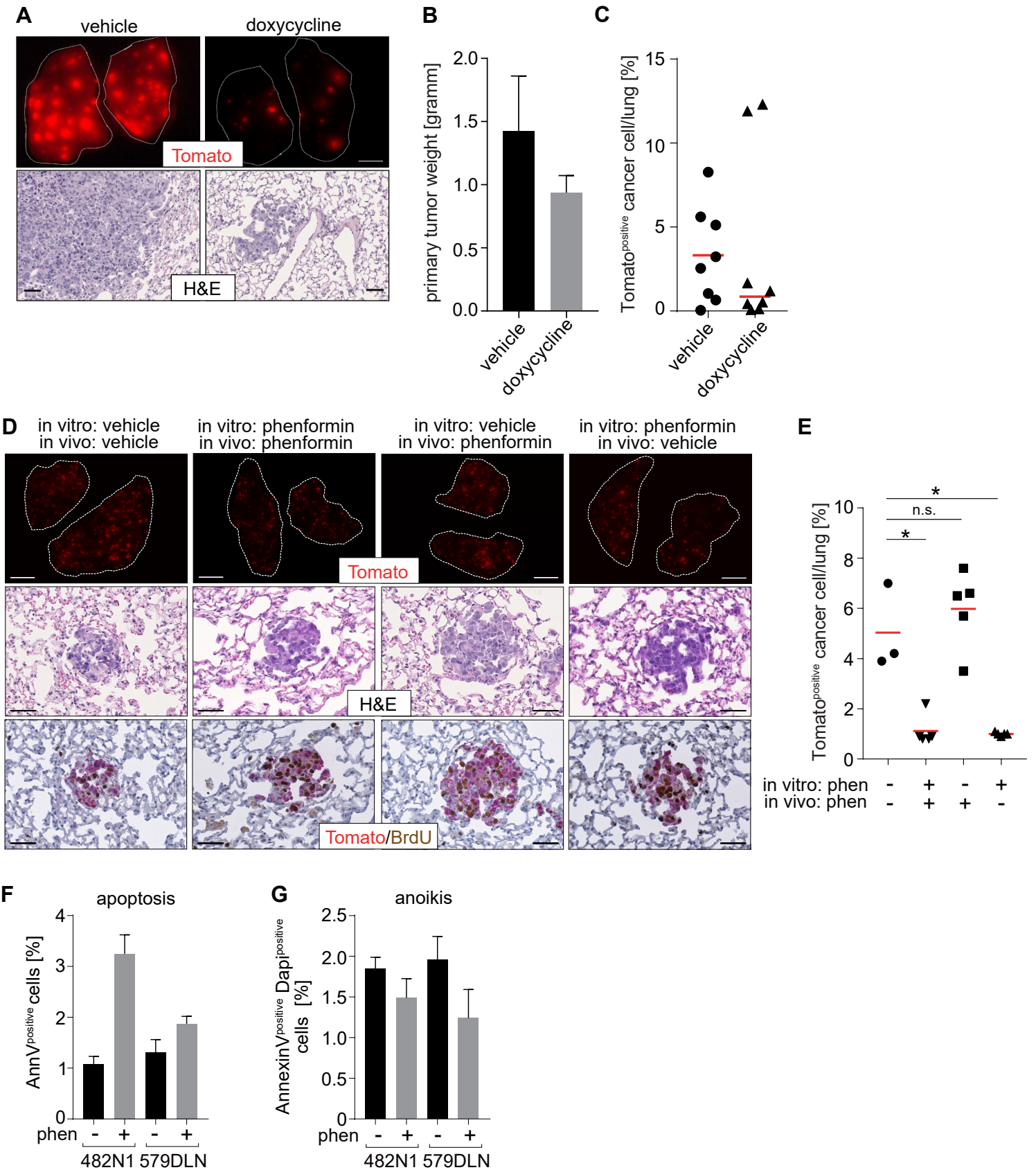
L. Western blot analysis of primary Met and T_{nonMet} cell lines for mitonuclear imbalance after 24 hours of treatment with control, doxycycline (Dox) or ethidium bromide (EtBr). No differences in expression of nuclear (Atp5, Uqcrc2 and Sdhb) or mitochondria encoded (mt-Co1) genes could be observed between T_{nonMet} and Met cell lines. One representative blot is shown, tested for 3 cell lines each.

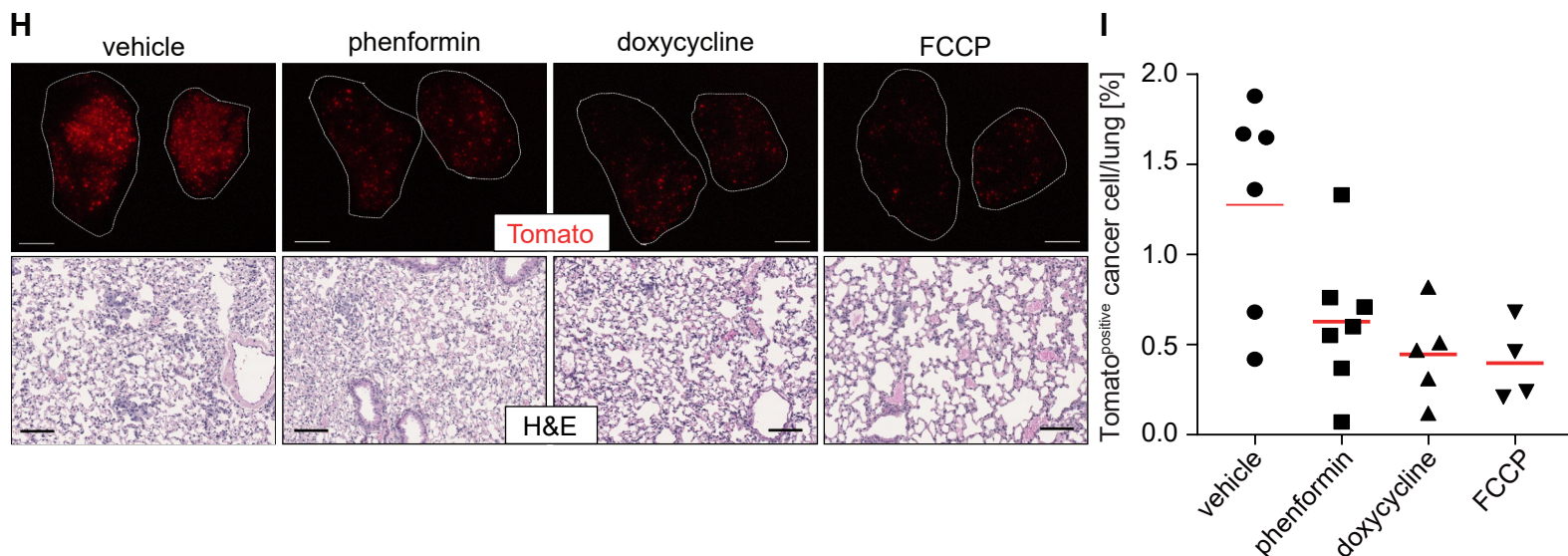
M. Western blot analysis of primary Met and T_{nonMet} cell lines for differential changes in signaling pathways due to phenformin (phen) treatment for 24 hours. No differences in expression levels between T_{nonMet} and Met cell lines could be detected. One representative blot out of three blots is shown, tested for 2 cell lines each.

N-Q Cell viability analysis with PrestoBlue assay. Cells were either treated with vehicle (black line), 200 µM phenformin (pink line), 50ng/ml ethidiumbromide (green line), or 15µg/ml doxycycline (blue line). No significant differences could be detected between the treated cells and their respective untreated controls. Two T_{nonMet} (**N,P**) and two Met (**O,Q**) cell lines were analyzed each tested in triplicate, each in three independent experiments. Error bars indicate SEM.

R-U. Analysis of migration in Met and T_{nonMet} cells at normoxic (**R,S**) and hypoxic (1 % O₂, **T,U**) conditions as well as at physiological (pH 7.4; **R,T**) or acidic (pH 6.5, **S,U**) conditions. Three independent experiments measured in triplicate, one representative experiment each is shown. Error bars indicate SEM.

V, W. Analysis of sphere forming capacity in T_{nonMet} and Met cells. (**V**) Exemplary pictures of one T_{nonMet} and one Met cell line on day 1 and day 8 of 3D sphere culture. (**W**) Quantification of growth in diameter from day 1 to day 8; One out of three independent experiments performed in triplicate for each three Met and three T_{nonMet} cell lines is shown. Error bars indicate SEM.





Supplementary Figure S5. Mitochondria of metastasis in *in vivo* mouse models of lung cancer have reduced functionality and are a target for anti-metastatic treatment.

A-C. Mice were subcutaneously injected with a metastatic lung cancer cell line and treated with either doxycycline (1 mg/kg i.p., $n = 8$ mice) or vehicle control ($n = 8$ mice) daily starting 9 days after injection. 29 days after injection, lungs were harvested and analyzed by fluorescent stereomicroscope (**A**, upper panel, scale bar = 1 mm) and H&E staining (**A**, lower panel, scale bar = 50 μm). (**B**) Primary tumor weight was slightly reduced in doxycycline-treated animals. (**C**) The percent of Tomato^{positive} cancer cells was reduced in 6 out of 8 doxycycline-treated animals. Each dot represents one sample, the red line indicates the median.

D, E. 579DLN Met cells were pretreated *in vitro* with phenformin (*in vitro* phen: 200 μM) or vehicle control for 48 hours and then intravenously injected into recipient mice. Mice were then treated with either phenformin (*in vivo* phen: 100 mg/kg p.o., $n = 5$ mice per group) or vehicle control ($n = 3$ or 5 mice, respectively) daily starting at the day of injection. 3 days after injection, lungs were harvested and analyzed by fluorescent stereomicroscope (**D**, upper panel, scale bar = 1 mm), H&E staining (**D**, middle panel, scale bar = 50 μm), and IHC for Tomato and BrdU (**D**, lower panel, scale bar = 50 μm) and flow cytometry (**E**). The percentage of Tomato^{positive} cancer cells in the lungs was significantly reduced upon pretreatment with phenformin (**E**, $*p < 0.05$, n.s. $p > 0.05$). Each dot represents one sample, the red line indicates the mean.

F. Analysis of apoptosis induction in two Met cell lines used for the *in vivo* transplantation experiments after treatment with phenformin (200 μM) or control. Three independent experiments measured in triplicate, one representative experiment is shown. Error bars indicate SEM.

G. Analysis of anoikis induction in two Met cell lines used for the *in vivo* transplantation experiments after treatment with phenformin (200 μM) or control. Three independent experiments measured in triplicate, one representative experiment is shown. Error bars indicate SEM.

H, I. 579DLN Met cells were pretreated *in vitro* with phenformin (200 μM), doxycycline (15 $\mu\text{g}/\text{ml}$), FCCP (2 μM), or vehicle control for 48 hours and then intravenously injected into recipient mice. 3 days after injection, lungs were harvested and analyzed by fluorescent stereomicroscope (**H**, upper panel, scale bar = 1 mm) and H&E staining (**H**, lower panel, scale bar = 100 μm) and flow cytometry (**I**). The percentage of Tomato^{positive} cancer cells in the lungs was significantly reduced upon pretreatment with phenformin ($p = 0.0002$). Each dot represents one sample, the red line indicates the mean.